



Land Surface Temperature Retrieval from LANDSAT 8 data using Emissivity Estimation: A case study of Bengaluru Urban

Dr. Shivanand Chinnappavar¹, Dr. Sawant Sushant Anil², Sasi M³

¹Associate Professor, Regional Institute of Education Mysuru, Karnataka

²Assistant Professor, School of Life Sciences,

JSS Academy of Higher Education and Research, Mysuru, Karnataka

³Research Scholar, School of Life Sciences,

JSS Academy of Higher Education and Research, Mysuru, Karnataka

Corresponding Author – Dr. Shivanand Chinnappavar

DOI- 10.5281/zenodo.13861008

Abstract:

The land surface temperature (LST) is a crucial variable in many fields, including studies of global climate change, urban land use and cover, geo- and biophysical modelling, and many more. Remote sensing studies of terrestrial processes now have many opportunities to study the land temperature using Landsat – 8 Operational Line Imager & Thermal Infrared Sensor (OLI & TIRS) satellite data. The Methods used to estimate the LST are Top of Atmosphere (TOA), Brightness temperature (BT), NDVI, Propagation of Vegetation, and Land surface Emissivity to compute the land surface temperature of Bengaluru urban (LSE). Regarding the Normalized Difference Vegetation Index (NDVI) values for various land use/land cover (LU/LC) types identified from the Landsat visible and NIR channels, the variability of retrieved LSTs has been examined. The process that uses the visible and near infrared bands has been used to determine the Land Surface Emissivity (LSE) values required to implement the method. The Present Study Exhibits the land surface temperature of Bengaluru Urban using five methods, as results shows 78.9 and 47.5 as high and low temperature respectively.

Keywords: LST, Land surface Emissivity, Normalized Difference Vegetation Index.

Introduction:

The temperature of a surface that can be detected when it is in direct contact with a measuring device is known as the Land Surface Temperature (LST). A crucial factor in the physics of land-surface processes at both the regional and global stages is land-surface temperature (LST), which combines the effects of all surface-atmosphere interactions and energy fluxes between the atmosphere and the ground(1,2). The skin temperature of the land surface is known as LST. Due to the simultaneous modification of natural land cover and introduction of urban materials, i.e. anthropogenic surfaces, global urbanisation has dramatically changed the landscape, which has important climatic effects across all scales. Due to the non-homogeneity of the land surface cover and other meteorological conditions, LST is generally used to identify and characterise Urban Heat Island (UHI)(3).

The Thermal Infrared Sensor and the Operational Land Imager (OLI) are the two sensors that are carried by LANDSAT 8. (TIRS). Eight bands in the visible, near-infrared, and shortwave infrared areas of the electromagnetic spectrum are used by OLI to collect data at a spatial resolution of 30m. An extra panchromatic band with a spatial resolution of 15m is also collected by OLI. Using two bands situated in the atmospheric window

between 10 and 12 m, TIRS detects the TIR radiance with a spatial precision of 100 m (4,5). Numerous methods have been devised to estimate LST for land cover dynamic monitoring using brightness temperature, meteorology, and climatology Single Channel Technique and Split Window Technique(6,7).

Using the Kalman filter strategy, geostationary satellites and platforms like SEVIRI (Spinning Enhanced Visible and Infrared Imager) can obtain surface emissivity and temperature simultaneously. When compared to LST from non-geostationary satellite observations, the retrieval method, which is physical in nature, provides very good findings for both land- and sea-surface temperatures. Different land cover types, including desert, agricultural, and vegetated areas, as well as urban areas and seas, can be found to generate extremely good results using the same Kalman filter process (8,9).

Mathematical notations of parameters involved in LST determination are found in literature with not-so-uniform expressions. In this paper, TToA, denotes the top-of-atmosphere (ToA, or at-sensor) brightness temperature for channels i ; LToA, is the ToA spectral radiance for channel i ; $B_i(T_i)$ is the ToA thermal radiance; ρ_λ , LS is the reflectance from the surface; LSE the Land Surface Emissivity for bands; and P_v is the proportion of

vegetation. Because of the stray light effect observed in band 11 images of Landsat 8 (10,11). The main objective of this paper to estimate the land surface temperature of Bengaluru urban using five mathematical steps.

Study Area and Methods:

1 Study Area:

The Indian state of Karnataka's Bangalore Urban district has the highest population density. It is bordered by the Krishnagiri district of Tamil Nadu on the south, the Ramanagara district on the west, and the Bangalore Rural district of Bangalore on the east and north. When the former Bangalore district was divided into the Bangalore Urban and Bangalore Rural districts in 1986, the Bangalore

Urban district was created. Hebbala (Bangalore North), Kengeri (Bangalore South), Krishnarajapura (Bangalore East), Yelahanka (Bangalore North Additional), and Anekal are the five taluks that make up Bangalore Urban.

The Bangalore Urban district's administrative centre is located in the city of Bangalore. The district is made up of two divisions, five talukas, seventeen hoblies, eight hundred and seventy-two villages, eleven rural habitations, five towns, one tier-three city, and one tier-one city. It is governed by 96 village panchayats, seventy-seven taluk panchayats, five town municipal councils, one city municipal council, and one city corporation (Mahanagara Palike).

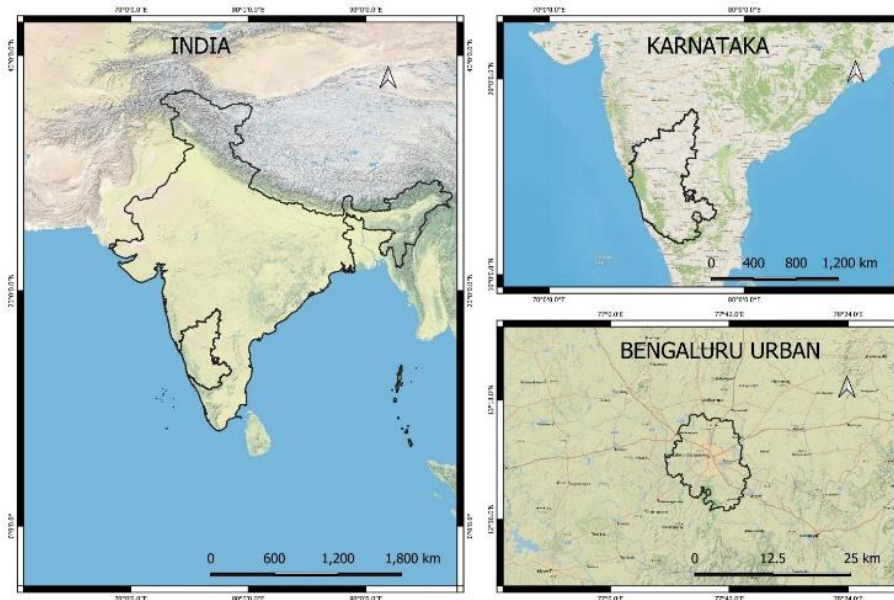


Figure 1: Study Area Map of Bengaluru Urban.

The district had a population of 6,537,124 of which 88.11% is urban as of 2001. As of Census 2011, its population has increased to 9,621,551, with a sex-ratio of 908 females/males, the lowest in the state and its density is 4,378 people per square km. The population of Bangalore Urban district in 2011 was 9,621,551, which is almost equivalent to the population of Belarus. As a result, it is ranked third

in India (out of a total of 640). 4,378 people live in the district per square kilometre (11,340 per square mile). Its population grew at a rate of 46.68% between 2001 and 2011. Bangalore has a literacy rate of 88.48% and a sex ratio of 908 females for every 1000 males. The population is made up of 12.46% scheduled castes and 1.98% scheduled tribes, respectively (12).

2 Data Sources:

Parameter	Resolution	Source
Landsat -8	30m	https://earthexplorer.usgs.gov/

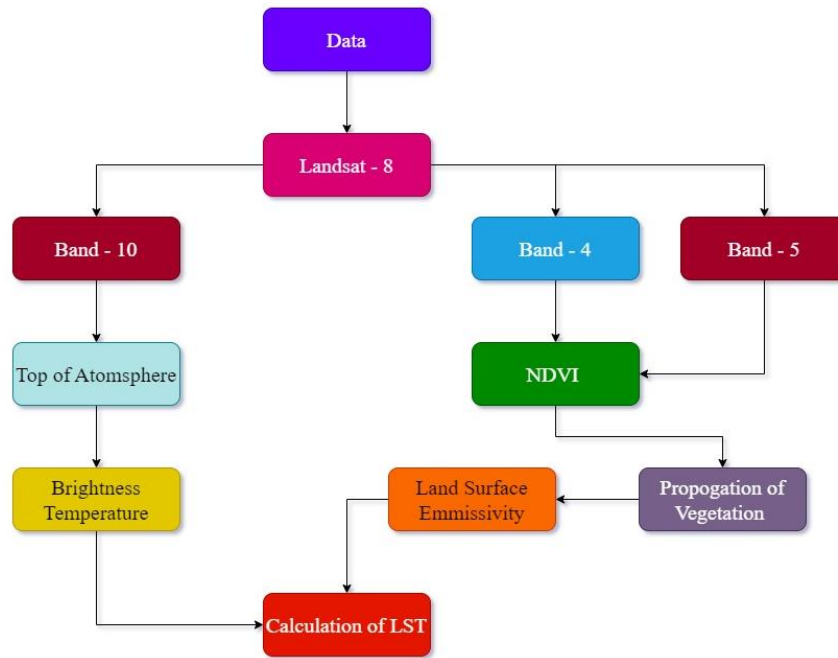


Figure 1 Research Methodology

3 Methodology:

4 Methods:

Step 1: Top of Atmosphere

The satellite data products were a set of data that had been geometrically adjusted. The initial phase of the proposed approach is to use the following equation to translate the band 10 DN (Digital Number) values to at-sensor spectral radiance (13,14).

$$TOA = M_L * Q_{cal} + A_L - Q_i$$

Where:

- L_λ = TOA spectral radiance (Watts/(m² * srad * μm))
- M_L = Band-specific multiplicative rescaling factor
- Q_{cal} = Quantized and calibrated standard product pixel values (DN)
- A_L = Band-specific additive rescaling factor
- Q_i = is the correction value for Band 10 of Landsat 8.

Step 2: Brightness Temperature:

The TIRS band data should be converted to brightness temperature (BT) using the thermal constants provided in the metadata file and the following equation after DN values have been converted to at-sensor spectral radiance.

$$BT = \frac{K2}{\ln(\frac{K1}{L_\lambda})} - 273.15$$

K1 and K2 are the TIR band 10 thermal constants, and their values can be found in the metadata file that goes with the satellite image. Absolute zero must be added in order to convert the data to Celsius, which is about equal to -273.15. The atmospheric effect is not taken into account when extracting the LST because the atmosphere in our research location is quite dry and the range of water vapour values is rather modest.

Step 3: NDVI Method for Emissivity Correction:

The Normalized Difference Vegetation Index (NDVI) is crucial for identifying the various types of land cover in the research area. The NDVI scale goes from -1.0 to +1.0. The normalised difference between the red band (0.64 -0.67 m) and near infrared band (0.85-0.88 m) of the photos is used to calculate NDVI on a per-pixel basis.

$$NDVI = \frac{NIR-RED}{NIR+RED}$$

where NIR is a pixel's value in the near infrared band and RED is its value in the red band. In order to compute proportional vegetation (Pv) and emissivity (ε), the NDVI must first be calculated.

Step 4: Calculate the proportion of Vegetation Pv:

The next step is to use the NDVI values from step 3 to determine proportional vegetation (Pv). This proportional vegetation provides an estimate of the area covered by each type of land cover. The proportions of vegetation and bare soil are obtained from the NDVI of clean pixels. NDVI values of 0.7 and 0.2 were proposed to be used in global situations. While the number for vegetated surfaces (NDVI= 0.5) may be too low in some circumstances, NDVI can approach 0.8 or 0.9 for higher resolution data on agricultural lands (15).

$$Pv = \left(\frac{NDVI - NDVI_s}{NDVI_v - NDVI_s} \right)^2$$

Step 5: Calculate Land Surface Emissivity (LSE) (ε)

Since land surface emissivity (LSE) is a proportionality factor that scales the black body radiance (Plank's law) to measure emitted radiance and it is the ability of transmitting thermal energy across the surface into the atmosphere, it must be calculated in order to estimate land surface temperature (LST). At the pixel scale, natural

surfaces are heterogeneous in terms of variation in LSE. The LSE also heavily depends on factors like vegetation type, surface roughness, and others (16).

$$\epsilon = 0.004 * P_v + 0.986$$

Where:

0.004 and 0.986 is constant values for Landsat images

P_v is the propagation of vegetation (Step 4)

Step 6: Calculation Land surface Temperature

The last step is to calculate LST using LSE obtained from P_v and NDVI and brightness temperature (BT) of band 10 in the calculation. Equation can be used to get LST (17,18).

$$T_s = \frac{BT}{\{1 + [\left(\frac{\lambda BT}{P}\right) \ln \epsilon \lambda]\}}$$

Where:

- B_t = Top of Atmosphere Brightness Temperature
- λ = wavelength-Emitted Radiance (λ is 10.895)
- ε Land surface Emissivity, Ref Step 5
- ρ = 1.438x10⁻² m k =14388
- ρ = $h \frac{c}{\sigma}$, c is Boltzmann Constant (1.38x10⁻²³ J/k), σ is the velocity of light (2.998x10⁴ m/s) and h is Planck's constant (6.626x10⁻³⁴ JS).

Result and Discussion:

Each dataset's NDVI is calculated following the conversion of the DN values to spectral radiances. The NDVI readings lie in the range of -1.0 to +1.0. That indicates that vegetation has

grown, which has an effect on the surface temperature. However, the NDVI for land cover types including built-up areas and bare terrain has not changed significantly. For the acquired satellite data, LSE were predicted to retrieve LST. The range of water vapour levels is rather modest in our research location because the atmosphere is comparably dry. Since the data obtained have convinced us, the atmospheric influence is not taken into consideration while estimating the LST.

urban heat island effect is noticeable because to the concentrated contiguous distribution. This might be as a result of the city's impermeable sub-surface's high solar radiation absorption rate. In addition, the city's tall and thick buildings, which severely obstruct air circulation and are not conducive to heat exchange, are combined with the high concentration of people and the heat that is released from human production activities. Together, these three factors are responsible for the city's greater temperature. The regions with cooler temperatures are primarily spread near water bodies or have more vegetation. The improvement of urban thermal development, reduction of the urban heat island effect, and regulation of the urban microclimate are all significant effects of increasing the plant cover in cities, as is well documented. The regions with cooler temperatures are primarily spread near water bodies or have more vegetation.

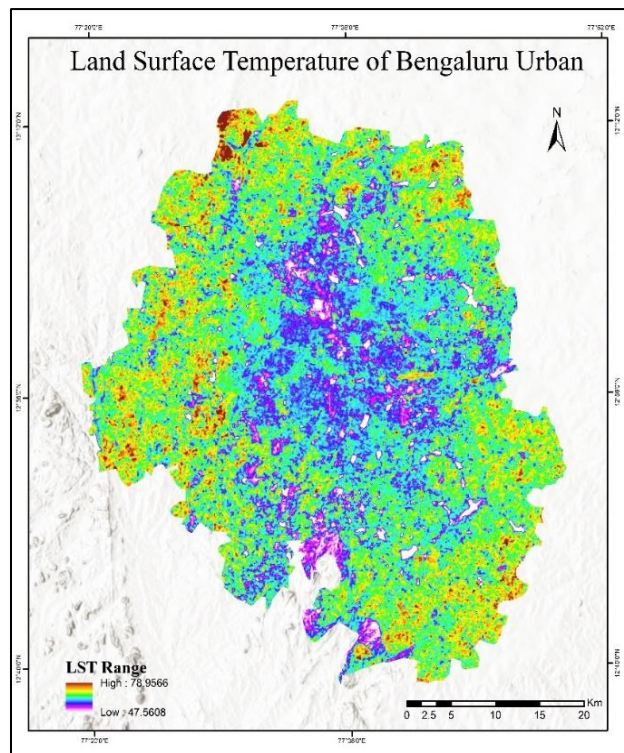


Figure 2 Land Surface Temperature of Bengaluru Urban District

The Landsat-8 TIRS data was given. For future Landsat-8 users and applications, the ability

to reliably calculate LST temperatures has obvious implications. Its superior thermal capabilities can

lead to new discoveries in earth science. TIRS's spatial resolution is reduced to 30 m, however the addition of two bands results in more precise LST calculations with TIRS than with its predecessor. The LST value of Bengaluru Urban ranges from 49.5 to 79.9, The final output map LST is Shown below.

Conclusion:

The Landsat-8 TIRS data was given. For future Landsat-8 users and applications, the ability to reliably calculate LST temperatures has obvious implications. Its superior thermal capabilities can lead to new discoveries in earth science. TIRS's spatial resolution is reduced to 30 m, however the addition of two bands results in more precise LST calculations with TIRS than with its predecessor. The comparison of the maximum, minimum, and average values of the six Methods retrieval results revealed that while there were some variances, the overall trend of the four methods' results over various time periods was quite comparable.

References:

1. Wan Z. A generalized split-window algorithm for retrieving land-surface temperature from space. *IEEE Transactions on Geoscience and Remote Sensing*. 1996;34(4):892–905.
2. Wan Z. New refinements and validation of the collection-6 MODIS land-surface temperature/emissivity product. *Remote Sens Environ*. 2014 Jan 1;140:36–45.
3. Joshi J, Bhatt B. ESTIMATING TEMPORAL LAND SURFACE TEMPERATURE USING REMOTE SENSING: A STUDY OF VADODARA URBAN AREA , GUJARAT. 2012;
4. Tomlinson CJ, Chapman L, Thornes JE, Baker C. Remote sensing land surface temperature for meteorology and climatology: a review. *Meteorological Applications* [Internet]. 2011 Sep 1 [cited 2023 Jan 24]; 18(3): 296–306. Available from: <https://onlinelibrary.wiley.com/doi/full/10.1002/met.287>
5. Jimenez-Munoz JC, Sobrino JA, Skokovic D, Mattar C, Cristobal J. Land Surface Temperature Retrieval Methods From Landsat-8 Thermal Infrared Sensor Data. *IEEE Geoscience and Remote Sensing Letters* [Internet]. 2014 [cited 2023 Jan 24];11(10):1840–3. Available from: https://www.academia.edu/6807763/Land_Surface_Temperature_Retrieval_Methods_From_Landsat_8_Thermal_Infrared_Sensor_Data
6. Jin M, Li J, Wang C, Shang R, Li ZL, Sobrino JA, et al. A Practical Split-Window Algorithm for Retrieving Land Surface Temperature from Landsat-8 Data and a Case Study of an Urban Area in China. *Remote Sensing* 2015, Vol 7, Pages 4371-4390 [Internet]. 2015 Apr 14 [cited 2023 Jan 24];7(4):4371–90. Available from: <https://www.mdpi.com/2072-4292/7/4/4371/htm>
7. Yu X, Guo X, Wu Z. Land Surface Temperature Retrieval from Landsat 8 TIRS—Comparison between Radiative Transfer Equation-Based Method, Split Window Algorithm and Single Channel Method. *Remote Sensing* 2014, Vol 6, Pages 9829-9852 [Internet]. 2014 Oct 15 [cited 2023 Jan 24];6(10):9829–52. Available from: <https://www.mdpi.com/2072-4292/6/10/9829/htm>
8. Masiello G, Serio C, Venafrà S, Liuzzi G, Göttsche F, Trigo IF, et al. Kalman filter physical retrieval of surface emissivity and temperature from SEVIRI infrared channels: A validation and intercomparison study. *Atmos Meas Tech*. 2015 Jul 29;8(7):2981–97.
9. Masiello G, Serio C, de Feis I, Amoroso M, Venafrà S, Trigo IF, et al. Kalman filter physical retrieval of surface emissivity and temperature from geostationary infrared radiances. *Atmos Meas Tech*. 2013 Dec 20;6(12):3613–34.
10. Malakar NK, Hulley GC, Hook SJ, Laraby K, Cook M, Schott JR. An Operational Land Surface Temperature Product for Landsat Thermal Data: Methodology and Validation. *ITGRS* [Internet]. 2018 Oct 1 [cited 2023 Jan 24];56(10):5717–35. Available from: <https://ui.adsabs.harvard.edu/abs/2018ITGRS..56.5717M/abstract>
11. Montanaro M, Gerace A, Lunsford A, Reuter D. Stray Light Artifacts in Imagery from the Landsat 8 Thermal Infrared Sensor. *Remote Sensing* 2014, Vol 6, Pages 10435-10456 [Internet]. 2014 Oct 29 [cited 2023 Jan 24];6(11):10435–56. Available from: <https://www.mdpi.com/2072-4292/6/11/10435/htm>
12. District Bangalore Urban, Government of Karnataka | Silicon Valley of India | India [Internet]. [cited 2023 Jan 24]. Available from: <https://bengaluruurban.nic.in/en/>
13. Barsi JA, Schott JR, Hook SJ, Raqueno NG, Markham BL, Radocinski RG. Landsat-8 Thermal Infrared Sensor (TIRS) Vicarious Radiometric Calibration. *Remote Sensing* 2014, Vol 6, Pages 11607-11626 [Internet]. 2014 Nov 21 [cited 2023 Jan 25];6(11):11607–26. Available from: <https://www.mdpi.com/2072-4292/6/11/11607/htm>
14. Wang F, Qin Z, Song C, Tu L, Karnieli A, Zhao S. An Improved Mono-Window Algorithm for Land Surface Temperature Retrieval from Landsat 8 Thermal Infrared Sensor Data. *Remote Sensing* 2015, Vol 7, Pages 4268-4289 [Internet]. 2015 Apr 10 [cited 2023 Jan 24];7(4):4268–89. Available from: <https://www.mdpi.com/2072-4292/7/4/4268/htm>

25];7(4):4268–89. Available from:
<https://www.mdpi.com/2072-4292/7/4/4268/htm>

15. Mallick J, Kant Y. Estimation of land surface temperature over Delhi using Landsat-7 ETM+. 2008;
16. Stathopoulou M, Cartalis C. Daytime urban heat islands from Landsat ETM+ and Corine land cover data: An application to major cities in Greece. *Solar Energy*. 2007 Mar 1;81(3):358–68.
17. Avdan U, Jovanovska G. Algorithm for automated mapping of land surface temperature using LANDSAT 8 satellite data. *J Sens [Internet]*. 2016 [cited 2023 Jan 25];2016. Available from:
https://www.researchgate.net/publication/296414003_Algorithm_for_Automated_Mapping_of_Land_Surface_Temperature_Using_LANDSAT_8_Satellite_Data